

# Use of tapered amplifier diode laser for biological-friendly high-resolution optical trapping

Wei Cheng,\* Ximiao Hou, and Fangmao Ye

Department of Pharmaceutical Sciences, College of Pharmacy, University of Michigan,  
428 Church Street, Ann Arbor, Michigan 48109, USA

\*Corresponding author: chengwe@umich.edu

Received June 2, 2010; revised July 24, 2010; accepted August 4, 2010;  
posted August 10, 2010 (Doc. ID 129366); published August 27, 2010

A 1064 nm laser is commonly used for biological optical trapping. However, it has the problem of generating reactive oxygen species in the presence of a sensitizer, which leads to photo damage in biological samples. Here we constructed optical tweezers using a tapered amplifier diode laser that operates at 830 nm. Compared to a 1064 nm laser, this laser is friendly to live cells, eliminates photo damage associated with reactive oxygen species, and allows simultaneous two-photon fluorescence imaging of green fluorescent proteins in live mammalian cells. All these advantages could significantly benefit future application of this single molecule technique in biological studies. © 2010 Optical Society of America

OCIS codes: 140.7010, 140.2020, 120.4640, 350.4855, 170.1420, 170.4520.

Since the first demonstration of stable optical trapping of micrometer-sized dielectric objects by Ashkin and coworkers [1], optical tweezers (OTs) have found increasing use in biochemical and biophysical investigations [2–4]. Recent technical advances further push the spatial resolution of OTs to the subnanometer regime [5–7], which allows observation of molecular motor activity at elementary steps [5,8]. However, the dual-trap design of OTs suffers from several problems associated with the choice of a 1064 nm laser. It heats up water [9] and forms a temperature gradient around the laser focus. Second, the silicon detector response to a 1064 nm laser is low-pass filtered due to the high transparency of silicon to wavelengths longer than 1  $\mu\text{m}$  [10]. Third, a 1064 nm laser excites molecular oxygen in aqueous solutions to produce reactive oxygen species (ROS) in the presence of a sensitizer [11]. ROS can introduce direct damage to nucleic acids, modifying bases and breaking the phosphodiester bonds [12].

We therefore decided to use a tapered amplifier (TA) diode laser (SYS-420-830-1000, Sacher LaserTechnik, LLC, Germany) that operates at 830 nm for construction of dual-trap OTs. We chose it for the following reasons: first, this wavelength minimizes the heating effect due to water absorption; second, 830 nm is very close to the peak sensitivity of silicon detectors; third, molecular oxygen has no absorption at 830 nm [13]. It is therefore not possible to produce ROS from this wavelength of laser irradiation. Indeed, two optimal wavelengths for laser trapping of live cells with minimal phototoxicity occur at 830 and 970 nm [14,15]. Meanwhile, a TA laser can provide sufficient power with decent beam quality, with  $M^2$  values of 1.3–1.5. It is therefore a good candidate for construction of dual-trap OTs.

The schematic layout of the OT instrument is shown in Fig. 1. The instrument is fully enclosed on an optical table and situated in a temperature-controlled room [16]. To obtain diffraction-limited beam profiles for quantitative optical trapping, we found it necessary to couple the TA laser to a single-mode optical fiber. The beam profile after fiber

coupling is very well described by a diffraction-limited Gaussian beam. We routinely obtain 50%–60% fiber coupling efficiency and achieve at least 500 mW of power at the end of the fiber. Half of this power offers 40 pN force for a 1.3  $\mu\text{m}$  polystyrene bead, sufficient for many purposes. We can trap polystyrene beads of 200 nm diameter. In addition, polystyrene beads of various diameters can be trapped with very good linearity for trap stiffness up to the trap escape force. This allows us to conveniently calibrate trap stiffness by using the power-spectrum fitting method [17].

Figure 2(a) shows the typical force-extension curves measured for a single RNA hairpin composed of 30 AU followed by 30 CG base pairs [18] using the 830 nm laser tweezers without addition of any oxygen scavenger systems [11,19]. Throughout the folding and refolding cycles of these hairpins, they showed expected patterns of transition without signs of photo damage. In contrast, at the

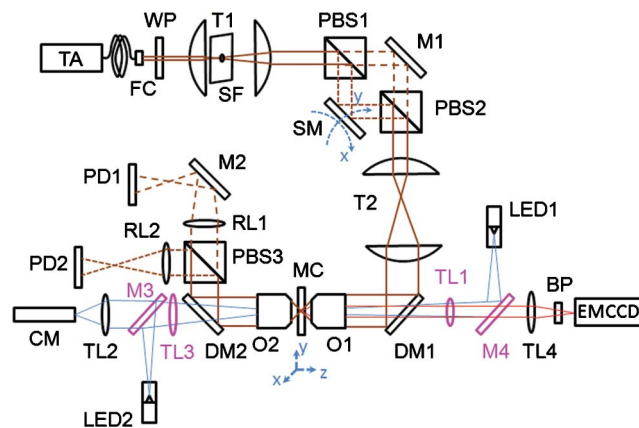


Fig. 1. (Color online) Schematic layout of the OT/TPF microscope using TA diode laser. FC, fiber collimator; WP, wave plate; T1, T2, telescopes; SF, spatial filter; PBS1, PBS2, PBS3, polarizing beam splitters; M1, M2, M3, M4, reflective mirrors; SM, steerable mirror; DM1, DM2, dichroic mirrors; O1, O2, objectives; MC, microfluidic chamber; TL1, TL2, TL3, TL4, tube lens; RL1, RL2, relay lens; PD1, PD2, position-sensitive detectors.

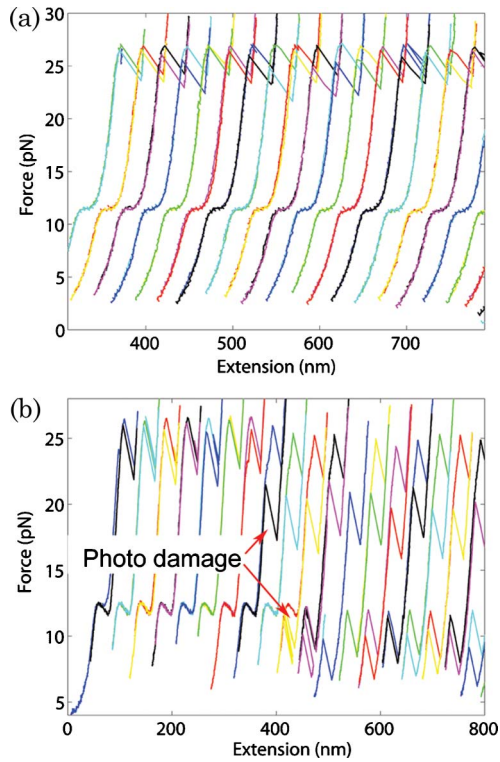


Fig. 2. (Color online) Consecutive cycles of force-extension measurements for a single RNA hairpin with (a) 830 and (b) 1064 nm OTs, respectively. The trajectories are arbitrarily shifted along the extension axis for clarity of display.

same laser power for a 1064 nm laser, when a single RNA molecule is unfolded by mechanical force to become single stranded, ROS can modify RNA bases and irreversibly change the folding and unfolding behavior of the molecule [Fig. 2(b)]. Moreover, we can routinely hold on a single molecule tether for 30 min, which is in dramatic contrast to the tether lifetime measured using 1064 nm laser tweezers (a few minutes or less) [11] at comparable laser power. These experiments have been performed using both 1.3  $\mu\text{m}$  and 860 nm diameter polystyrene beads, and no sign of singlet oxygen induced damage was observed.

To test whether this 830 nm laser is friendly to mammalian cells, we freshly cultured T lymphocytes and op-

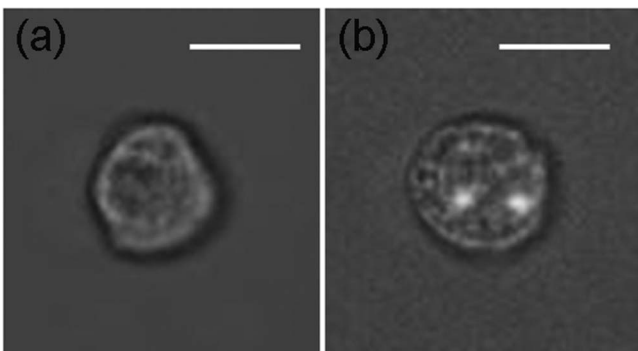


Fig. 3. Optical trapping of T lymphocytes in a solution containing amine-reactive green fluorescent dye, where a freshly cultured T cell is shown in (a) and a heat-killed T cell is shown in (b). The observation was repeated for a total of ten cells. The scale bars are 10  $\mu\text{m}$ .

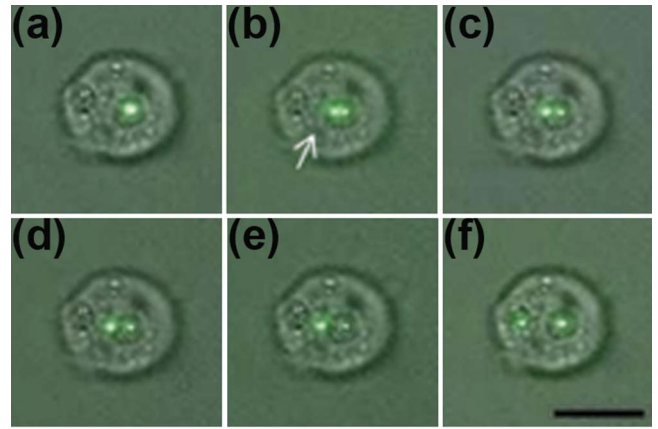


Fig. 4. (Color online) Overlap of bright-field and TPF images of a single 293T cell trapped by a 830 nm laser. Initially, (a) two laser beams were at the same focus, then one beam was moved away [the left focus in (b), indicated by arrow] from the other until they were 5.7  $\mu\text{m}$  apart, in (f). Scale bar is 10  $\mu\text{m}$ .

tically trapped a single cell in a buffered solution containing amine-reactive fluorescent dyes [Fig. 3(a)]. We then monitored the two-photon fluorescence (TPF) [20] of the dye excited by the same 830 nm trapping laser using the electron-multiplying CCD. The live cell can be trapped for over 2 h without any fluorescence emission from the interior of the cell. However, for a control dead cell [Fig. 3(b)], within 5 min of trapping in the dye solution, strong TPF from the dye was visible throughout the cell, indicating that the cell membrane was permeable and dye molecules penetrated to the interior of the cell. The above results indicate that, for a freshly cultured T lymphocyte, even over a time course of several hours, the cell remains alive under intense laser irradiation.

One added benefit of using a 830 nm laser for OTs is that this wavelength allows two-photon excitation of green fluorescent proteins (GFPs) [21]. To demonstrate this capability, we transfected 293T cells with a plasmid that expresses enhanced GFPs (EGFPs) in the cytosol and then optically trapped a single cell for fluorescence examination (Fig. 4). Throughout the laser scanning process, EGFP fluorescence can always be detected, although the intensity varies with locations inside the cell. We also confirmed the two-photon excitation of EGFPs by trapping and imaging giant liposomes that encapsulated purified EGFPs (data not shown).

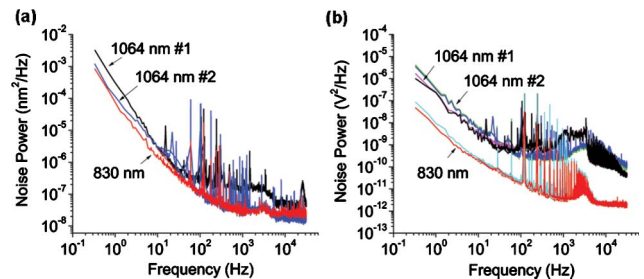


Fig. 5. (Color online) 830 nm TA laser has lower-intensity noise than a 1064 nm laser. Power spectra of (a) laser pointing noise; and (b) laser intensity noise. For each laser, the intensity noise for two traps are shown, 830 nm in red and cyan, and two 1064 nm lasers in black and purple, blue and green respectively.

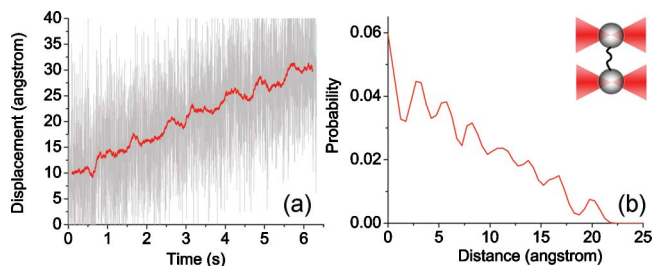


Fig. 6. (Color online) Spatial resolution of the OT instrument measured using BFP interferometry. (a) The displacement between two beads was measured as a function of time; (b) pairwise distance analysis of the red filtered data shown in (a).

To quantitate the signal-to-noise features of this OT instrument, we measured laser pointing and intensity noise using position-sensitive silicon detectors. These measurements were conducted after laser noise had been optimized. Although the laser pointing stability is about the same level for both lasers [Fig. 5(a)], the intensity noise of the TA laser [Fig. 5(b)] is 1 order of magnitude lower than that of a 1064 nm laser, 0.01% over a time scale of 5 min. This is an important advantage. It will decrease the noise from the beads' Brownian motion. In addition, we measured the spatial resolution of the instrument based on the published method [6] by tethering a single DNA molecule between two polystyrene beads (1.3  $\mu\text{m}$  in diameter). We steered one of the traps through the mirror (SM in Fig. 1) installed on a nanopositioning stage to increase the tension on the molecule in a stepwise manner, and used backfocal plane (BFP) interferometry to measure the displacement between two beads [22]. Figure 6(a) shows one such example, where the gray represents data measured at 625 Hz and the red solid curve is raw data boxcar filtered to 5 Hz. A displacement between two beads at a 3 Å interval, as shown by the pairwise distance analysis for the same data [Fig. 6(b)], can be measured with a tension of 5 pN on the molecule. This is by far the lowest force reported for angstrom-level resolution with a "dumb-bell" optical trap [5,6], to the best of our knowledge.

In summary, we have constructed a dual-trap OT instrument that can detect angstrom-level displacement using a TA diode laser. The choice of a 830 nm laser wavelength eliminated the photo damage associated with the generation of ROS. The low-intensity noise of the laser offers angstrom-level spatial resolution on a second time scale, which will be useful for high-resolution single molecule manipulation studies. In addition, mammalian cells can be trapped by the high-power laser for hours without apparent cell death. Simultaneous TPF excitation of GFPs paves the way for future single molecule studies in the context of a live cell, for example, manipulation of a single receptor on the cell surface and measurement of a reporter gene expression to probe the mechanisms of mechanotransduction.

We thank Edwin Vedejs in the Chemistry Department for sharing the use of a rotary evaporator to make liposomes. We thank Spherotech Inc. (Lake Forest, IL) for kindly providing 200 nm polystyrene beads. W. C. thanks start-up funding support from the University of Michigan and also thanks Carlos Bustamante and Jeffrey Moffitt, with whom the problems of 1064 nm lasers were first identified. The following reagents were obtained through the AIDS Research and Reference Reagent Program, Division of AIDS, National Institute of Allergy and Infectious Diseases (NIAID), National Institutes of Health (NIH): Sup-T1 cell line from James Hoxie; pEGFP-Vpr from Warner C. Greene.

## References

1. A. Ashkin, J. M. Dziedzic, J. E. Bjorkholm, and S. Chu, *Opt. Lett.* **11**, 288 (1986).
2. L. Bai, T. J. Santangelo, and M. D. Wang, *Annu. Rev. Biophys. Biomol. Struct.* **35**, 343 (2006).
3. W. J. Greenleaf, M. T. Woodside, and S. M. Block, *Annu. Rev. Biophys. Biomol. Struct.* **36**, 171 (2007).
4. J. R. Moffitt, Y. R. Chemla, S. B. Smith, and C. Bustamante, *Annu. Rev. Biochem.* **77**, 205 (2008).
5. E. A. Abbondanzieri, W. J. Greenleaf, J. W. Shaevitz, R. Landick, and S. M. Block, *Nature* **438**, 460 (2005).
6. J. R. Moffitt, Y. R. Chemla, D. Izhaky, and C. Bustamante, *Proc. Natl. Acad. Sci. USA* **103**, 9006 (2006).
7. A. R. Carter, Y. Seol, and T. T. Perkins, *Biophys. J.* **96**, 2926 (2009).
8. J. R. Moffitt, Y. R. Chemla, K. Aathavan, S. Grimes, P. J. Jardine, D. L. Anderson, and C. Bustamante, *Nature* **457**, 446 (2009).
9. E. J. G. Peterman, F. Gittes, and C. F. Schmidt, *Biophys. J.* **84**, 1308 (2003).
10. K. Berg-Sorensen, L. Oddershede, E. L. Florin, and H. Flyvbjerg, *J. Appl. Phys.* **93**, 3167 (2003).
11. M. P. Landry, P. M. McCall, Z. Qi, and Y. R. Chemla, *Biophys. J.* **97**, 2128 (2009).
12. M. D. Evans, M. Dizdaroğlu, and M. S. Cooke, *Mutat. Res.* **567**, 1 (2004).
13. C. Long and D. Kearns, *J. Chem. Phys.* **59**, 5729 (1973).
14. H. Liang, K. T. Vu, P. Krishnan, T. C. Trang, D. Shin, S. Kimel, and M. W. Berns, *Biophys. J.* **70**, 1529 (1996).
15. K. C. Neuman, E. H. Chadd, G. F. Liou, K. Bergman, and S. M. Block, *Biophys. J.* **77**, 2856 (1999).
16. C. Bustamante, Y. R. Chemla, and J. R. Moffitt, *CSH Protoc.* **2009**, pdb ip73 (2009).
17. K. C. Neuman and S. M. Block, *Rev. Sci. Instrum.* **75**, 2787 (2004).
18. W. Cheng, S. Dumont, I. Tinoco, Jr., and C. Bustamante, *Proc. Natl. Acad. Sci. USA* **104**, 13954 (2007).
19. M. T. Woodside, W. M. Behnke-Parks, K. Larizadeh, K. Travers, D. Herschlag, and S. M. Block, *Proc. Natl. Acad. Sci. USA* **103**, 6190 (2006).
20. Y. Liu, G. J. Sonek, M. W. Berns, K. Konig, and B. J. Thromberg, *Opt. Lett.* **20**, 2246 (1995).
21. P. T. So, C. Y. Dong, B. R. Masters, and K. M. Berland, *Annu. Rev. Biomed. Eng.* **2**, 399 (2000).
22. F. Gittes and C. F. Schmidt, *Opt. Lett.* **23**, 7 (1998).